



Green Synthesis of Zinc Oxide Nanoparticles and their Antibacterial Properties using Plant Extract of *Aristolochia elegans*

JUHI AGGARWAL* and TANVEER ALAM

Department of Chemistry, K.L. DAV P.G. College, Roorkee-247667, India

*Corresponding author: E-mail: aggarwaljuhi1990@gmail.com

Received: 5 May 2020;

Accepted: 7 July 2020;

Published online: 25 September 2020;

AJC-20074

Present paper deals with the synthesis of zinc oxide nanoparticles (ZnONPs) using leaf extract of *Aristolochia elegans* and study of antibacterial property for some human bacterial pathogens. The ZnONPs synthesized were characterized using UV-Vis, FT-IR, XRD, EDX, TEM and SEM techniques. The synthesized ZnONP having a crystallite size of 20.1 nm exhibited a distinct absorption peak maxima at 358 nm. The ZnONPs synthesized using the extract of *A. elegans* have shown antibacterial activity against *M. luteus*, *S. aureus* (Gram-positive), *E. coli* and *P. aeruginosa* (Gram-negative).

Keywords: Green synthesis, ZnO nanoparticles, Antimicrobial activity, *Aristolochia elegans*.

INTRODUCTION

In the 21st century, nanotechnology overcome as the fast-growing interdisciplinary area of scientific research that has a valuable impact on many sectors like medicine, biotechnology, electronics, photonic [1,2], biomedical areas [3], nano-diagnostics [4,5], antimicrobials [6], luminescence [7] and photocatalytic potential [8], etc. The nanoparticles have unique chemical and physical properties in terms of the shape, size, surface characteristic and inner structure by just increasing the ratio of surface area per volume of material. This will allow nanoparticles to have characteristics like a well-defined larger segment of surface atoms, reduced structures, more surface charge an energy, enhanced solubility, chemical composition and better surface morphology.

Mostly, two methods have been reported for the synthesis of the nanoparticles *i.e.* chemical and physical methods, such as sol-gel [9], hydrothermal [10], spray pyrolysis [11], microwave-assisted techniques [12], chemical vapour deposition [13], ultrasonic condition [14], precipitation methods [15] and biosynthesis or green synthesis methods, such as plant extract, microbiological mediated [16]. The chemical method has the drawbacks of high cost, labour-intensive, generation of toxic by-products that are hazardous

to the environment and living beings and a high intake of energy for synthesis that may cause biological risks. The latter, biosynthesis or green synthesis, offers a unique, reliable, environment-friendly, non-toxic and overall an alternate process for the synthesis of nanoparticles having enhanced shape and size with a better environment-friendly method [17]. The popularity of the use of biosynthesized nanoparticles is very high as they have low-cost, ease in synthesis by changing the morphology to get unique chemical and physical properties, enhanced environmental capabilities, high solubility, enhanced biocompatibility and absence of various high toxic stabilizers.

In recent years, researchers focus on different metal oxide nanoparticles, *i.e.*, TiO₂, ZnO, CuO and Fe₃O₄, about their biological activities [18]. Within the large family of metal oxides, green ZnONPs become very popular due to its multi-functional behaviour and dynamic antimicrobial activity [19,20]. ZnO has exhibited tremendous advantages in the field of today's cutting-edge technologies [21,22]. Plants components such as leaves, stems, seeds, roots and fruits are primarily used in the synthesis of ZnONPs as extracts due to presence of high amount of phytochemicals, which are used as reducing and stabilizing agents. Specific biomolecules present in the plant extract have been shown to reduce metal ions to nano-sized material by a single-step approach.

Aristolochia elegans Mast. is a slender, woody perennial climber used as ornamental plants in several parts of the world [23]. In India, this plant habitat in the colder regions, *i.e.*, higher altitude regions. In present work, the ZnONPs were synthesized via the green synthesis method using the leaf extracts of *A. elegans*. The synthesized ZnONPs using *Aristolochia elagens* were studied for structural properties using Fourier-transform infrared (FT-IR) spectroscopy and X-ray diffraction (XRD) techniques. Further, the size, grain size, size distribution and morphology samples were also analyzed by using different characterization techniques.

EXPERIMENTAL

All the reagents and solvents were of analytical grade and used without any further purification. Zinc nitrate and sodium hydroxide pellets with 99.9% and 99% purity, respectively, were purchased from Sigma-Aldrich Chemicals, USA. The fresh and healthy leaves of *Aristolochia elegans* were collected from Pantanjali Herbal Garden, Patanjali Yogapeeth, Haridwar, India, which was authentication by the appropriate taxonomist and Head of Department, Herbal Research Department, Patanjali Yogapeeth, Haridwar, India.

Preparation of plant extract: The collected fresh and healthy leaves of plants were thoroughly washed with tap water, then with distilled water and kept for shed drying for 15 days. The dried leaves were grounded and powder of the leaves of each plant was made. About 10 g of powder collected into a flask containing 100 mL of double distilled water and heated at 60-80 °C for 1 h. The resultant leaf extract was allowed to cool under room temperature, then filtered with the Whatman filter paper No. 1. The final extract was kept at 4 °C for further experiments.

Green synthesis of ZnONPs: For the green synthesis of the ZnONPs, 90 nM of an aqueous solution of zinc nitrate and the aqueous leaf extract were stirred at 120 °C for 2 h. 2 M Sodium hydroxide solution was added dropwise into the mixture to maintain the pH value at 12. The resultant white precipitates were washed with distilled water, followed by ethanol to remove the remaining impurities and dried in an oven 250 °C for 4 h. The dried solid was then stored in the refrigerator for the characterization.

Characterization: The UV-Vis spectral analysis was done using UV-Vis spectrometer (Perkin-Elmer lambda 19) at the wavelength of 200-800 nm. Absorption measurement of different samples having the same material has been documented to check the concentration level of nanoparticles during the UV-Vis spectra analysis. To investigate the crystalline properties such as average particle size, its nature and dimensions, the X-ray diffraction analysis was also performed. Fourier transform infrared (FTIR) spectroscopic analysis was performed using a Perkin-Elmer spectrum RX-1 IR spectrophotometer within the ranging from 4000 to 400 cm^{-1} . Surface morphology like shape, size, dispersed nature of nanoparticles and elemental composition of the synthesized sample was determined by EDX spectrometer analysis followed by scanning electron microscopy (SEM). To visualize the grain size, distribution of the green synthesized nanoparticles, transmission electron micro-

scopy (TEM) with Model JEM 2100 (JEOL, Japan) was used. The average particle size was analyzed by the Image J Software and a Histogram of size distribution was displayed using origin Software.

The ZnONPs were examined for antimicrobial activity using Agar well diffusion method against clinical isolates (*Micrococcus luteus*, *Escherichia coli*, *Staphylococcus aureus*, *Pseudomonas aeruginosa*, *Streptococcus pneumoniae*) individually. The bacterial pathogens were separately inoculated into the flask containing nutrient broth (20 mL) and incubated for 37 °C for 24 h. After incubation, bacterial suspension was prepared aseptically with a turbidity equivalent to 0.5 M McFarland solution. The bacterial suspension (75 μL each) was spread on Muller-Hinton Agar plates. Four wells in each plate were punched in the above MHA plates with a sterile corkborer (6mm diameter). Nanoparticle suspensions were prepared in DMSO (1% v/v). Now, 75 μL of each suspension was filled into the respective agar wells and the plates were then incubated at 37 °C for 48 h. Further, the same activity will be done by using 100 μL of bacterial suspension. Zone of inhibition (mm) for both (75 & 100 μL) was recorded for antimicrobial activity.

RESULTS AND DISCUSSION

The mixture of aqueous leaf extract of leaves and zinc nitrate was observed to change in its colour from yellowish-brown colour to pale white colour after 24 h of incubation in the dark. This change in colour is summarily the indicative of formation of ZnONPs. It has been shown that the change in colour occurs due to the surface plasma resonance effect. Further, ZnO synthesized using *A. elagens* extract were studied for the structural properties and antibacterial studies.

UV-vis analysis: The synthesized sample was analyzed under the UV-vis spectroscopy. The absorption spectrum was determined at the wavelength ranging from 200-800 nm. The strong electronic absorption was obtained at 358 nm (Fig. 1), corresponding to the pronounced quantum confinement effect in the ZnO particles [24]. ZnONPs have high excitation binding

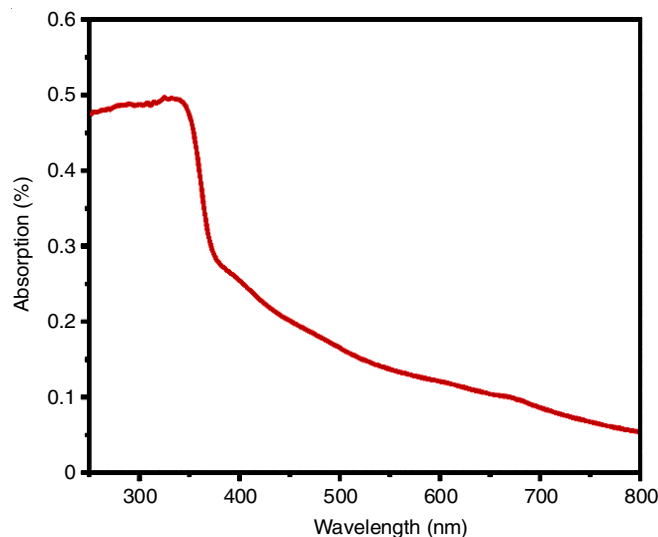


Fig. 1. UV-vis spectra of biosynthesized ZnONPs

energy at room temperature, which formed a distinct peak centered at 350 nm [25].

FT-IR analysis: The FTIR spectra of ZnONPs exhibited the characteristic vibrational signals at 3421, 2922, 1649, 1539, 1445, 1084, 780, 527 and 468 cm^{-1} . A broad peak of 3421 cm^{-1} corresponds to the O–H stretching vibrations due to the presence of the water molecules. The C–H stretching vibration of the phenolic group was observed at 2922 cm^{-1} , while a peak of 1649 attributed to the C=O stretching vibration of primary amines. The vibrational peaks at 1539 and 1445 cm^{-1} showed symmetric and asymmetric stretching of $-\text{C}=\text{C}=\text{C}$ bond, respectively. The C–N stretching vibration was found at 1084 cm^{-1} , while the peak at 527 and 468 cm^{-1} exhibited the characteristic stretching vibrational signals of ZnONPs (Fig. 2). These vibrational peaks indicate that the plant extract contains phenols, polyphenols and primary amines, which took part in the reduction, capping and finally stabilization of ZnONPs. Similar observations of phytochemical assisted synthesis of nanoparticles have also been made elsewhere [26].

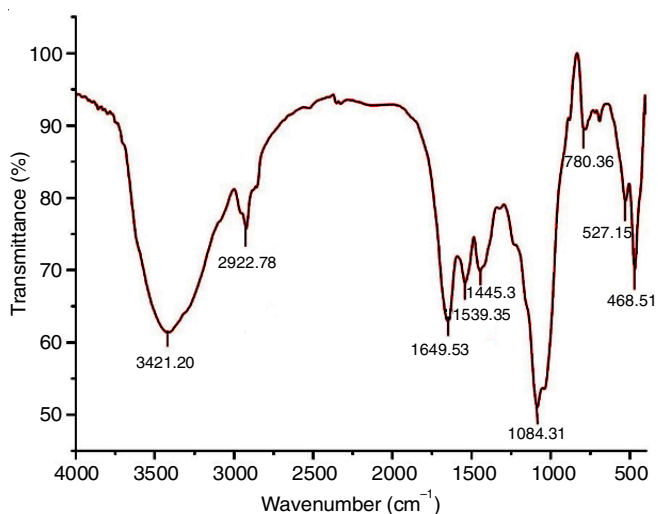


Fig. 2. FT-IR spectra of biosynthesized ZnONPs

Polyphenols are important biomolecules present in leaf extract of *A. elegans*, possibly responsible for the synthesis of ZnONPs. The process involves the ionization of zinc-nitrate in an aqueous medium to give Zn^{2+} , which then reduces to ZnO and thus aggregates as ZnONPs by polyphenols present in plant extract [27]. Alkaloids in the plant extract have been

shown to act as stabilizing agents, whereas the flavonoids act as capping agents.

XRD analysis: The X-ray diffraction analyses helps to determine the crystal lattice, phases and the planes of the nanoparticles. In present study, the diffraction peaks observed at 2θ values of 31.83°, 34.43°, 36.31°, 47.59°, 56.71°, 62.91°, 68.91° and 77.10° corresponds to the Bragg's lattice plane of (100), (002), (101), (102), (110), (103), (112) and (202), respectively, with respect to "hkl" values (Fig. 3). The obtained planes in the diffraction pattern of ZnONPs confirmed the +2-oxidation state of zinc. Also, the diffraction pattern matched well with the JCPDS card number 36-1451 [28]. The average crystalline size of the ZnONPs calculated using Debye Scherer's

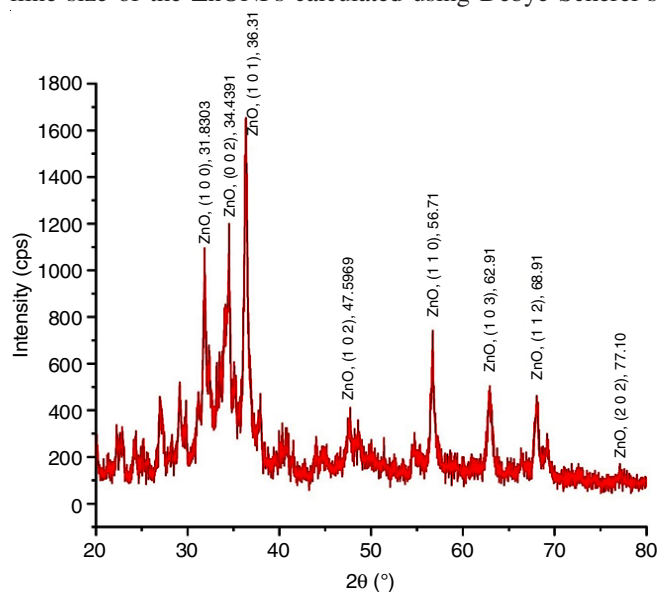


Fig. 3. XRD pattern of ZnONPs of leaf extract of *A. elegans*

formula was found to be 23.72 nm. The crystal structure of the ZnONPs was observed to be wurtzite hexagonal, as has also been reported elsewhere [29].

EDX and SEM analysis: Fig. 4(a) demonstrates the characteristic peaks of zinc at around 1 keV and for oxygen at approximately 0.5 keV under EDX analyses, which confirms the formation of ZnO. Fig. 4(b) showed the wt.% distribution of elements present in the nanomaterial. A sharp peak for carbon indicate scapping structures formed due to biomolecules pertaining to leaf extracts. Fig. 4(c) depicts SEM image of ZnONPs synthesized using leaf extract of *A. elegans*. Further-

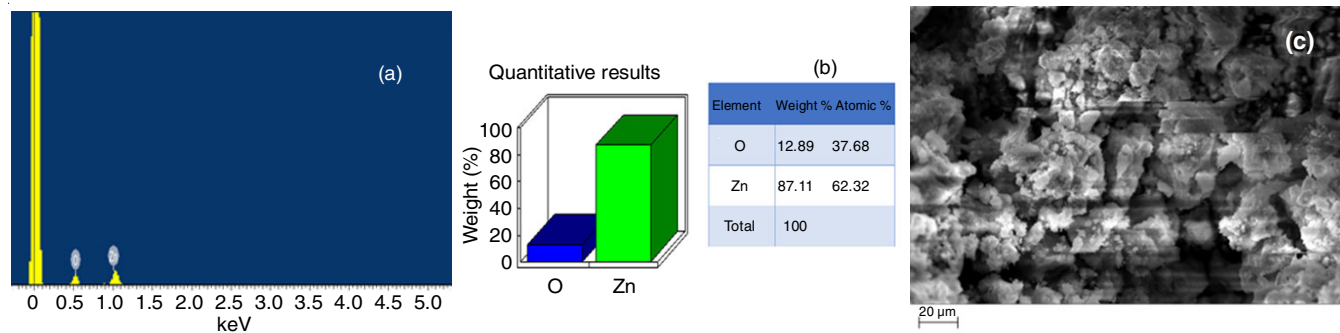


Fig. 4. (a) EDX pattern of ZnONPs, (b) Weight% distribution of elements in ZnONPs, (c) SEM analysis of ZnONPs

TABLE-1
ANTIBACTERIAL ACTIVITY (ZONE OF INHIBITION) BY ZnONPs SYNTHESIZED USING EXTRACT OF LEAVES OF THE *A. elegans*

| Pathogens | 75 μ L (synthesized ZnONP) | 100 μ L (synthesized ZnONP) | Standard (erythromycin) |
|--------------------------------|--------------------------------|---------------------------------|-------------------------|
| <i>Micrococcus luteus</i> | 22 \pm 0.5 | 24 \pm 0.5 | 23 \pm 0.5 |
| <i>Escherichia coli</i> | 16 \pm 0.5 | 18 \pm 0.5 | – |
| <i>Staphylococcus aureus</i> | 11 \pm 0.5 | 13 \pm 0.5 | 25 \pm 0.5 |
| <i>P. aeruginosa</i> | 10 \pm 0.5 | 12 \pm 0.5 | 11 \pm 0.5 |
| <i>Streptococcus pneumonia</i> | – | – | 20 \pm 0.5 |

more, the particles were observed to be highly agglomerated, which might be due to subsequent centrifugation and heating of the samples for SEM preparations.

TEM analysis: HR-TEM images described the microstructure and inter-planar distances of ZnONPs (Fig. 5a and 5b). It shows the rough imperfection of the ZnONPs (Fig. 5a). The interplanar distances of the planes were 0.25 nm and 0.30 nm corresponds to (100) and (101) planes, which are in good agreement with the diffraction pattern of ZnONPs. The SAED pattern of ZnO revealed that the synthesized catalyst was polycrystalline with small bright dots, which correspond to a small crystalline nature (Fig. 5c). The EDX pattern of the ZnO exhibited that the 57.9 wt.% of Zn and 42.1 wt.% of O were present in synthesized ZnONPs (Fig. 5d).

Antibacterial activity: The antibacterial activity of the synthesized ZnONPs was checked against clinical isolates such as *Micrococcus luteus*, *Escherichia coli*, *Staphylococcus aureus*, *Pseudomonas aeruginosa* and *Streptococcus pneumoniae*. The antibacterial activity against Gram-positive and Gram-negative bacterial isolates expressed in diameter of zone of inhibition (mm) at two different volumes of ZnONPs are shown in Table-1. ZnONPs showed a remarkable inhibition zone of 24 \pm 0.5, 18 \pm 0.5, 13 \pm 0.5 and 12 \pm 0.5 mm for *M. luteus*, *E. coli*, *S. aureus* and *P. aeruginosa*. No inhibition was however, observed against *S. pneumoniae*. Interestingly, *E. coli* was inhibited by the ZnONPs, which was resistant to erythromycin. Besides, the ZnONPs have shown antibacterial activity comparable to erythromycin against *M. luteus* and *P. aeruginosa*.

The ZnO nanoparticles have been characterized with significant antimicrobial activity. Present study suggested that

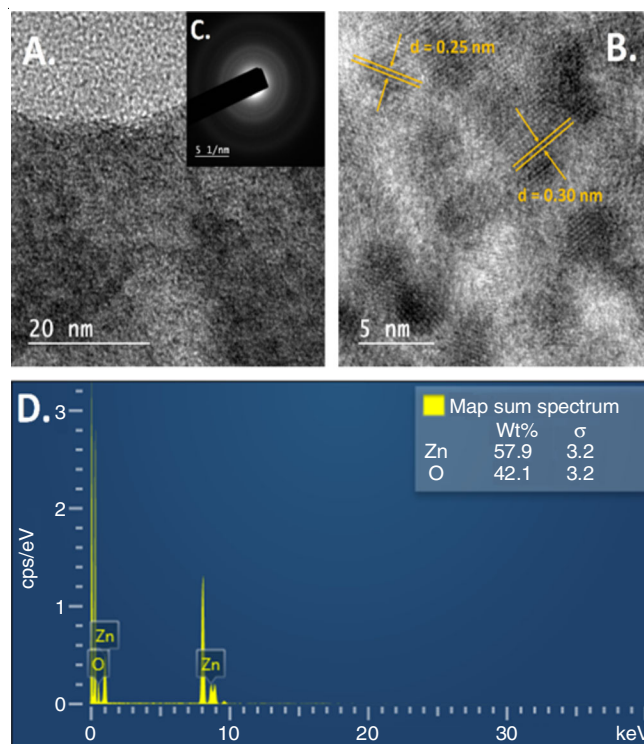


Fig. 5. (a & b). TEM images, (c). SAED pattern and (d). EDX pattern of ZnONPs of leaf extract of *A. elegans*

ZnONPs holds potential for antibacterial activities against both the Gram-positive and Gram-negative bacteria. The antibacterial activity of ZnONPs comparable to other reports are summarized in Table-2.

TABLE-2
COMPARISON OF ZnONPs SYNTHESIZED USING EXTRACT OF DIFFERENT PLANTS AND ANTIBACTERIAL ACTIVITY

| Plant name | Plant part | Shape | Size (nm) | Antibacterial activity | Inhibition zone (mm) | Ref. |
|----------------------------|------------|---------------------|-----------|-------------------------------------|----------------------|------|
| <i>Rubia cordifolia</i> | Leaf | Nano sheets | 23.61 | <i>Micrococcus luteus</i> | 25.00 | [30] |
| | | | | <i>Escherichia coli</i> | 14.00 | |
| | | | | <i>Staphylococcus aureus</i> | 17.00 | |
| <i>Catharanthus roseus</i> | Leaf | Spherical | 50.73 | <i>P. aeruginosa</i> | 11.10 | [31] |
| | | | | <i>E. coli</i> | 11.13 | |
| | | | | <i>P. mirabilis</i> | 11.15 | |
| | | | | <i>S. aureus</i> | 11.75 | |
| | | | | <i>S. pyogenes</i> | 11.53 | |
| | | | | <i>B. cereus</i> | 11.50 | |
| <i>Catharanthus roseus</i> | Leaf | Spherical | 23-57 | <i>P. aeruginosa</i> | 13.00 | [32] |
| | | | | <i>S. aureus</i> | 12.00 | |
| | | | | <i>E. coli</i> | 10.00 | |
| | | | | <i>Bacilu</i> | 12.00 | |
| <i>Aloe vera</i> | Leaf | Rod shaped | 500 | <i>E. coli</i> | 7.00 | [33] |
| | | | | <i>S. aureus</i> | 4.50 | |
| <i>Hibiscus subdariffa</i> | Leaf | Spherical, dumbbell | 16-60 | <i>S. aureus</i> and <i>E. coli</i> | – | [34] |

Conclusion

Present study reported the synthesis of ZnONPs from the leaf extract of *Aristolochia elegans* and evaluated for the biological activities.

CONFLICT OF INTEREST

The authors declare that there is no conflict of interests regarding the publication of this article.

REFERENCES

1. E. Redel, P. Mirtchev, C. Huai, S. Petrov and G.A. Ozin, *ACS Nano*, **5**, 2861 (2011); <https://doi.org/10.1021/nn103464r>
2. Z. Surowiec, M. Budzyński, K. Durak and G. Czernel, *Nukleonika*, **62**, 73 (2017); <https://doi.org/10.1515/nuka-2017-0009>
3. A.P. Ramos, M.A.E. Cruz, C.B. Tovani and P. Ciancaglini, *Biophys. Rev.*, **9**, 79 (2017); <https://doi.org/10.1007/s12551-016-0246-2>
4. P. Jamdagni, P. Khatri and J.S. Rana, *Int. Nano Lett.*, **6**, 139 (2016); <https://doi.org/10.1007/s40089-015-0177-0>
5. D. Bobo, K.J. Robinson, J. Islam, K.J. Thurecht and S.R. Corrie, *Pharm. Res.*, **33**, 2373 (2016); <https://doi.org/10.1007/s11095-016-1958-5>
6. S. Ahmed, M. Ahmad, B.L. Swami and S. Ikram, *J. Adv. Res.*, **7**, 17 (2016); <https://doi.org/10.1016/j.jare.2015.02.007>
7. N. Thovhogi, E. Park, E. Manikandan, M. Maaza and A. Gurib-Fakim, *J. Alloys Compd.*, **655**, 314 (2016); <https://doi.org/10.1016/j.jallcom.2015.09.063>
8. A. Eslami, M.M. Amini, A.R. Yazdanbakhsh, A. MohseniBandpei, A.A. Safari and A. Asadi, *J. Chem. Technol. Biotechnol.*, **91**, 2693 (2016); <https://doi.org/10.1002/jctb.4877>
9. K. Omri, I. Najeh, R. Dhahri, J. El Ghoual and L. El Mir, *Microelectron. Eng.*, **128**, 53 (2014); <https://doi.org/10.1016/j.mee.2014.05.029>
10. R. Dobrucka and J. Dlugaszewska, *Indian J. Microbiol.*, **55**, 168 (2015); <https://doi.org/10.1007/s12088-015-0516-x>
11. H.A. Salam, R. Sivaraj and R. Venkatesh, *Mater. Lett.*, **131**, 16 (2014); <https://doi.org/10.1016/j.matlet.2014.05.033>
12. D. Suresh, R.M. Shobharani, P.C. Nethravathi, M.A. Pavan Kumar, H. Nagabhushana and S.C. Sharma, *Spectrochim. Acta A Mol. Biomol. Spectrosc.*, **141**, 128 (2015); <https://doi.org/10.1016/j.saa.2015.01.048>
13. K. Vimala, S. Sundarraj, M. Paulpandi, S. Vengatesan and S. Kannan, *Process Biochem.*, **49**, 160 (2014); <https://doi.org/10.1016/j.procbio.2013.10.007>
14. V. Sáez and T.J. Mason, *Molecules*, **14**, 4284 (2009); <https://doi.org/10.3390/molecules14104284>
15. K. Elumalai, S. Velmurugan, S. Ravi, V. Kathiravan and S. Ashokkumar, *Mater. Sci. Semicond. Process.*, **34**, 365 (2015); <https://doi.org/10.1016/j.mssp.2015.01.048>
16. P.P. Gan and S.F.Y. Li, *Rev. Environ. Sci. Biotechnol.*, **11**, 169 (2012); <https://doi.org/10.1007/s11157-012-9278-7>
17. H. Agarwal, S.V. Kumar and S. Rajeshkumar, *Resource-Effic. Technol.*, **3**, 406 (2017); <https://doi.org/10.1016/j.reffit.2017.03.002>
18. S. Stankic, S. Suman, F. Haque and J. Vidic, *J. Nanobiotechnol.*, **14**, 73 (2016); <https://doi.org/10.1186/s12951-016-0225-6>
19. A. Sirelkhatim, S. Mahmud, A. Seeni, N.H.M. Kaus, L.C. Ann, S.K.M. Bakhori, H. Hasan and D. Mohamad, *Nano-Micro Lett.*, **7**, 219 (2015); <https://doi.org/10.1007/s40820-015-0040-x>
20. P.G. Krishna, P.P. Ananthaswamy, T. Yadavalli, N.B. Mutta, A. Sannaiah and Y. Shivanna, *Mater. Sci. Eng. C*, **62**, 919 (2016); <https://doi.org/10.1016/j.msec.2016.02.039>
21. C. Dagdeviren, S.-W. Hwang, Y. Su, S. Kim, H. Cheng, O. Gur, R. Haney, F.G. Omenetto, Y. Huang and J.A. Rogers, *Small*, **9**, 3398 (2013); <https://doi.org/10.1002/smll.201300146>
22. V. Anbukkarasi, R. Srinivasan and N. Elangovan, *Int. J. Pharm. Sci. Rev. Res.*, **33**, 110 (2015).
23. Y. Park, Y.N. Hong, A. Weyers, Y.S. Kim and R.J. Linhardt, *IET Nanobiotechnol.*, **5**, 69 (2011); <https://doi.org/10.1049/iet-nbt.2010.0033>
24. G. Yong, F. Gu, D. Han, Z. Wang and G. Guo, *J. Nanomater.*, **2010**, 289173 (2010); <https://doi.org/10.1155/2010/289173>
25. M. Mohammadian, Z. Eshaghi and S. Hooshmand, *J. Nanomed. Res.*, **7**, 00175 (2018); <https://doi.org/10.15406/jnmr.2018.07.00175>
26. R. Yuvakkumar, J. Suresh, B. Saravanakumar, A.J. Nathanael, S.I. Hong and V. Rajendran, *Spectrochim. Acta A Mol. Biomol. Spectrosc.*, **137**, 250 (2015); <https://doi.org/10.1016/j.saa.2014.08.022>
27. T. Bhuyan, K. Mishra, M. Khanuja, R. Prasad and A. Varma, *Mater. Sci. Semicond. Process.*, **32**, 55 (2015); <https://doi.org/10.1016/j.mssp.2014.12.053>
28. F. Fan, Y. Feng, P. Tang, A. Chen, R. Luo and D. Li, *Ind. Eng. Chem. Res.*, **53**, 12737 (2014); <https://doi.org/10.1021/ie501825t>
29. M. Darroudi, Z. Sabouri, R.K. Oskuee, A.K. Zak, H. Kargar and M.H.N. Abd Hamid, *Ceram. Int.*, **40**, 4827 (2014); <https://doi.org/10.1016/j.ceramint.2013.09.032>
30. Prachi, A. Mushtaq and D.S. Negi, *Asian J. Chem.*, **31**, 385 (2019); <https://doi.org/10.14233/ajchem.2019.21602>
31. M. Gupta, R.S. Tomar, S. Kaushik, R.K. Mishra and D. Sharma, *Front. Microbiol.*, **9**, 2030 (2018); <https://doi.org/10.3389/fmicb.2018.02030>
32. G. Bhumi and N. Savithramma, *Int. J. Drug Dev. Res.*, **6**, 208 (2014).
33. J.L. Venkataraju, *J. Biochem. Technol.*, **3**, 151 (2014).
34. N. Bala, S. Saha, M. Chakraborty, M. Maiti, S. Das, R. Basu and P. Nandy, *RSC Adv.*, **5**, 4993 (2015); <https://doi.org/10.1039/C4RA12784F>